JMEPEG (2007) 16:284–292
DOI: 10.1007/s11665-007-9049-8

1059-9495/$19.00

Development of Accurate Constitutive Models for Simulation of Superplastic Forming

Hari Raman, George Luckey, Ghassan Kridli, and Peter Friedman

(Submitted December 12, 2006; in revised form January 30, 2007)

Superplastic forming (SPF) has been considered a process for improving the formability of aluminum alloys for the production of automotive body panels. In order to accurately simulate the SPF process, elevated temperature, uniaxial tension tests are used to develop the material flow model. Due to the high temperature and large degree of deformation in these tests, strain is typically calculated using crosshead displacement rather than with an extensometer. This approach requires the assumption of a constant material volume in the gage section to calculate the uniform strain. It has been observed that a significant amount of material flows from the grips into the gage section during testing which results in inaccuracies in the material model. This article presents a numerical tool that accounts for material flow from the grips and produces a more accurate constitutive equation. Experimental and numerical validations of the results of the developed tool are presented.

Keywords aluminum sheet, finite element analysis, material model, superplastic forming

1. Introduction

One of the enabling technologies for expanding the use of superplastic forming is finite element analysis (FEA). FEA plays an important role in die design, the prediction of optimum pressure cycles for minimum forming time and material selection. The ability of the simulation code to predict the deformation behavior of the material is a key factor in developing optimal gas pressure cycles that can form the part in the least time. Much of this ability comes from an accurate constitutive model that characterizes the material behavior. A constitutive model attempts to define the deformation characteristics in the form of a stress-strain-strain rate relationship coupled with other factors related to the microstructure and micromechanics of deformation.

The parameters of the constitutive equation are typically derived by performing a number of high temperature uniaxial tension tests on the material. The stress-strain data is fit to the constitutive model to obtain the coefficients of the equation. The high operating temperature and the large values of deformation in these tensile tests make it difficult to use extensometry to monitor the strain in the gage section of the specimen. Therefore, strain and strain rate are typically calculated from the crosshead displacement. Due to the low flow stresses at elevated temperatures, material flows from the grip region into the gage section of the tensile specimen thus introducing a considerable error in all subsequent calculations that are used to derive the parameters of the material constitutive equation. The resulting constitutive equation fails to characterize the material accurately. Thus, there is a need for accurate material constitutive equations which will lead to accurate simulation results; thus allowing for higher confidence in simulation results and the ability to numerically optimize the process.

A list of constitutive models based on different deformation mechanisms was compiled by Chandra (Ref 1). While these models are comprehensive in characterizing the material, they require extensive testing and microstructural investigation that is too time consuming for industrial applications where new materials must be rapidly evaluated. Therefore, the power law model (shown in Eq 1) is typically used, and has been shown to lead to relatively accurate results (Ref 2, 3).

$$\sigma = K\dot{\varepsilon}^m\varepsilon^n \qquad \text{(Eq 1)}$$

where σ is the flow stress, ε is the strain, and $\dot{\varepsilon}$ is the strain rate. K, m and n are the coefficients of the constitutive equation; where K is the strength coefficient, n is the strain hardening exponent, and m is the strain rate sensitivity factor.

2. High Temperature Tensile Test

2.1 Experimental Setup

Superplastic tensile tests on the AA5083 alloy were conducted using an MTS Sintech Machine (MTS Systems Corporation, Eden Prairie, MN) equipped with a three zone split furnace that maintains the specimen at superplastic temperatures. The load frame was equipped with an 8.9 KN load cell and the data acquisition was controlled by a computer. A photograph of the test equipment is shown in Fig. 1.

This article was presented at Materials Science & Technology 2006, Innovations in Metal Forming symposium held in Cincinnati, OH, October 15-19, 2006.

Hari Raman and **Ghassan Kridli,** University of Michigan-Dearborn, 4901 Evergreen Road, Dearborn, MI 48128; **George Luckey** and **Peter Friedman,** Ford Research and Innovation Center, 2101 Village Rd., Dearborn, MI 48121. Contact e-mail: sluckey@ford.com.

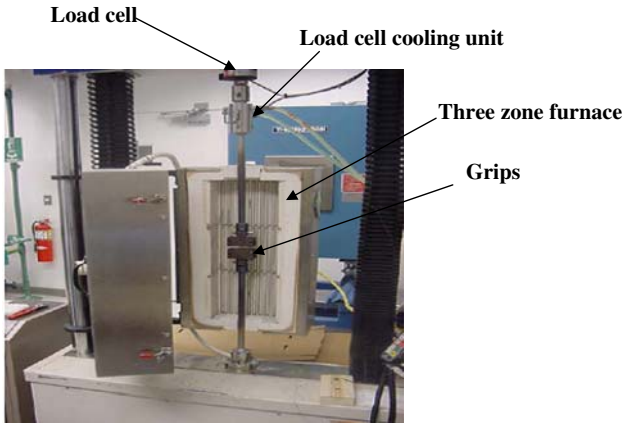

Fig. 1 Tensile test frame equipped with 3-zone split furnace and an 8.9 kN load cell (Ref 4)

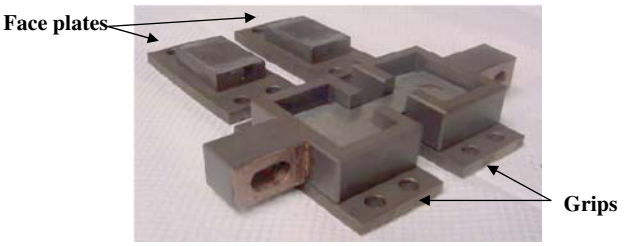

Fig. 2 Inconel grips with tensile specimen (Ref 4)

The grips that hold the tensile specimen (Fig. 2) were made from Inconel in order to withstand superplastic testing temperatures. Face plates clamp down on the specimen grip ends to constrain material flow from the grips, and the grips pull the tensile specimen by gripping the shoulders. The short gage length is characteristic of tensile specimens used in superplastic studies. The specimen has sharp transition radii from the grip to the gage to limit grip flow.

2.2 Experimental Procedure

The testing procedure begins by loading the tensile sample into the Inconel grips. The faceplates are clamped down on the grip ends of the tensile specimen. All the fasteners that are part of the Inconel grips are coated with a copper lubricant to allow easy removal after exposure to elevated temperatures. Once the samples have been mounted on the grips, the setup is then fastened to the pull rods of the MTS load frame.

Before the start of the test the specimens were subjected to a 90 min heating cycle in order achieve a stable target temperature of 475 °C. An initial crosshead velocity was applied based on a target value of initial strain rate. When the specimen elongation reached 5%, the velocity of the crosshead was changed based on a second value of target strain rate. This type of a test is called a 'jump test' and can be used to calculate a materials strain rate sensitivity. In this work, an alternative method was applied to calculate the strain rate sensitivity of the material (*m*-value) which is described in Section 2.3.

The tensile tests that were performed as part of this work were all constant crosshead speed tests (except for the discrete jump in strain rate at 5% strain). The initial strain rates ranged from 1×10^{-4}/s to 4×10^{-2}/s. The tests were all 'jump tests' with the exception of two, one with an initial strain rate of 1×10^{-3}/s and the other, a 3×10^{-3}/s test. The test details are included in the test matrix (Table 1).

2.3 Strain rate Sensitivity

Prior to analytical calculations, the strain rate sensitivity of the material was determined from experimental data. The strain rate sensitivity (*m*-value) of a material is defined as the rate of change of flow stress with change in strain rate. The relation is given by Eq 2.

$$m = \frac{\partial \ln \sigma}{\partial \ln \dot{\varepsilon}} \qquad \text{(Eq 2)}$$

where m is the strain rate sensitivity, σ is the flow stress, and $\dot{\varepsilon}$ is the strain rate. The strain rate sensitivity was calculated by comparing two tensile tests of different initial strain rate. The tensile data from both tests were compared at equal tensile elongations. The cross-sectional areas of the two tensile specimens corresponding to the two tests were assumed to be equal for the same tensile elongation to yield Eq 3.

$$m = \frac{\ln \frac{P_2}{P_1}}{\ln \frac{CHS_2}{CHS_1}} \qquad \text{(Eq 3)}$$

In Eq 3, P_1 and P_2 are the flow loads and CHS_1 and CHS_2 are the crosshead velocities that correspond to the tests.

Two tensile tests were conducted for each condition in Table 1. The average load and CHS for each test condition corresponding to 10% tensile elongation were applied in Eq 3 to calculate an *m*-value. This *m*-value was assumed to represent the average *m* between the initial strain rates of the tensile tests used in the calculation. An *m*-value was established using each set of load and CHS data and all other data sets having a greater initial strain rate. This resulted in a total of 35 *m*-values which were then plotted as a function of average log strain rate ($\log \dot{\varepsilon}$) as shown in Fig. 3. A linear equation was fit to the data and was used to calculate an *m*-value for a particular initial strain rate. A linear fit was chosen because the range of strain rates that was being studied was not wide enough to represent the classic bell shaped curve that is typical of superplasticity, but fell within a portion that can be approximated with a linear fit. Using this linear equation the *m*-values calculated corresponded to the initial strain rate of each tensile test are tabulated in Table 2. These values were used in the developed analytical model used to correct for grip flow and for establishing the values of K and n.

3. Constitutive Coefficient Development

3.1 Analytical Model

The material flow can be observed by testing a tensile specimen with a 2.5 mm grid etched on to the surface. As can be seen from the tested specimen in Fig. 4, material is pulled into the gage region which introduces error into the calculation of strain and strain rate. An analytical method was developed to account for the material flow phenomenon, calculate corrected values of strain and strain rate and refine the coefficients of the constitutive equation.

Table 1 Matrix of superplastic tensile tests

Test no.	Material	Temperature	Strain rate #10	Strain rate #2, s^{-1}	CHS#1, mm/s	CHS#2, mm/s
1.	AA5083	475	1.0×10^{-4}	2.0×10^{-4}	0.00222	0.00222
2.*	AA5083	475	1.0×10^{-3}	1.0×10^{-3}	0.0222	0.0222
3.*	AA5083	475	1.0×10^{-3}	2.0×10^{-3}	0.0222	0.04662
4.*	AA5083	475	3.0×10^{-3}	3.0×10^{-3}	0.0666	0.0666
5.*	AA5083	475	3.0×10^{-3}	4.0×10^{-3}	0.0666	0.0932
6.*	AA5083	475	5.0×10^{-3}	6.0×10^{-3}	0.111	0.1399
7.	AA5083	475	7.0×10^{-3}	8.0×10^{-3}	0.155	0.1865
8.	AA5083	475	9.0×10^{-3}	1.0×10^{-2}	0.1998	0.2331
9.	AA5083	475	1.0×10^{-2}	2.0×10^{-2}	0.222	0.4662
10.	AA5083	475	3.0×10^{-2}	4.0×10^{-2}	0.666	0.9324

* Tensile tests performed to evaluate constitutive coefficients K and n

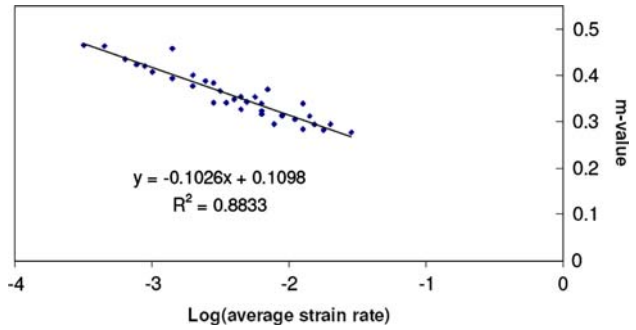

Fig. 3 Plot showing m-value as a function of log strain rate (Ref 2)

Table 2 Calculated m-values from the linear equation fit (Fig. 3)

Strain rate, s^{-1}	m-Value
0.001	0.42
0.002	0.39
0.003	0.37
0.004	0.36
0.006	0.34

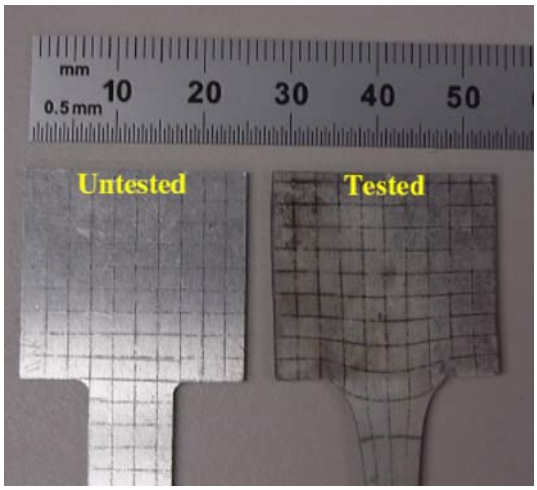

Fig. 4 Tensile samples before and after testing with 2.5 mm etched grid (Ref 2)

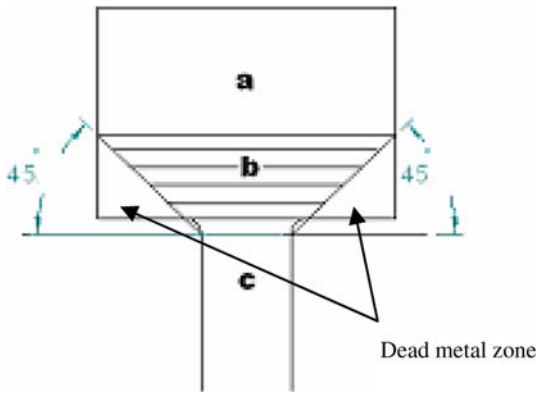

Fig. 5 Analytical slab model indicating a trapezoidal region in the grip that feeds material into the gage section

The analytical model shown in Fig. 5 uses slab analysis to calculate stress levels in the gage based on the applied load and an initial guess of constitutive parameters. This is performed by dividing the tensile specimen into three sections, (a), (b), and (c) (Fig. 5). Section-c represents the gage of the specimen. The trapezoidal section (b) was assumed to feed all the material that flows in from the grips and the material in section (a) was assumed to undergo no elongation; this was confirmed by observation of the grids on tested tensile specimens. The two triangular sections that fall outside the trapezium on either side were assumed to be dead metal zones. This assumption was made by drawing parallels to plane strain metal extrusion and studying the material flow characteristics of that process.

The trapezoidal section was constructed using basic geometry. The tensile samples have corner radii of 1.6 mm between the gage and the grip sections. Two 45° lines were constructed from the end points of the radii at the gage and the points of intersection with the grips were joined to obtain the trapezoidal section. This section was further divided into ten equally spaced sections.

The analytical method involved a sequence of mathematical calculations to arrive at corrected values of strain and strain rate. The inputs used were the experimental load data, the crosshead velocities and the adjusted initial dimensions of the tensile specimen to account for the thermal expansion during the 90 min heat up cycle. Initial estimates of K and n were used with an m-value that was previously determined for a particular initial strain rate. The model was based on imposing a condition of load balance on the trapezoidal grip section, along the axial

direction of the specimen. Before the load frame crosshead moved and the trapezoidal section underwent elongation, the stress in each of the ten sections was calculated based on the load and initial cross-sectional area. Once the crosshead displaced through a certain distance and the section started to elongate, the new cross-sectional areas were calculated based on the strain to account for reduction in width and thickness. The strain rate was calculated based on the constitutive equation (Eq 1). To calculate the strain in any of the ten divisions for a specific displacement of the crosshead, the strain rate was integrated over the time interval that had elapsed. The new cross-sectional area was then calculated based on the strain value in order to calculate the stress value for the next load step and the same calculations were repeated to find the strain values in each of the ten divisions. The sum of the elongation of all the ten sections gave the total elongation of the trapezoid. The elongation of the trapezoidal region quantifies the material flow from the grips of the tensile sample. The calculated elongation of the trapezoid was doubled to account for the two grips of the tensile sample. The resulting value was subtracted from the crosshead displacement to obtain the actual elongation of the material in the gage at each load step in the tensile data and update the strain in the gage section.

The corrected strain rate was calculated by modifying an equation of "velocity balance" Eq 4 (Ref 3). The equation sums up the velocities of the material displacement in the gage and the grip sections to yield the crosshead velocity of the load frame.

$$\mathrm{CHS} = l_a e^{\varepsilon a}\dot{\varepsilon}_a + l_c e^{\varepsilon c}\dot{\varepsilon}_c + \sum l_b e^{\varepsilon b}\dot{\varepsilon}_b G_b \qquad \text{(Eq 4)}$$

where l, ε and $\dot{\varepsilon}$ are initial length, strain, and strain rate, respectively. The subscripts a, b, and c refer to the different sections shown in Fig. 5. The value of '*b*' ranges from 1 to 10 where the number corresponds to a particular division in the trapezoidal grip region. G_b is a geometric factor given by $w_b t_b / w_c t_c$where w and t are instantaneous width and thickness and the subscripts b and c refer to the corresponding section in Fig. 5. In this work, section-a was assumed to undergo negligible elongation; therefore the first term in Eq 4 was dropped and the resulting equation was rearranged as shown in Eq 5 to calculate the corrected strain rate in the gage.

$$\dot{\varepsilon}_c = \frac{\mathrm{CHS} - \sum l_b e^{\varepsilon b}\dot{\varepsilon}_b G_b}{l_c e^{\varepsilon c}} \qquad \text{(Eq 5)}$$

The steps followed to calculated corrected values of strain and strain rate were based on initial values of K and n that ignored flow from the grips and the calculated m-value. These initial values of K and n were obtained by curve fitting the constitutive equation to uncorrected values of strain and strain rate.

To refine (or adjust) the constitutive equation parameters to account for grip flow, an iterative approach that involved minimization of sum of squares was adopted. The corrected values of strain were used to calculate the cross-sectional area of the gage for each load step. The flow stress in the gage was then calculated using the load values from the tensile data. Flow stress values were also calculated using the constitutive equation [Eq 1]. A minimization of sum of squares was performed to calculate new values of K and n. The m-value was not altered because it was desired that this coefficient be based solely on experimental data because it is the most important coefficient in FEA for predicting thickness profile.

The new values replaced the initial values of K and n in the analytical method to further refine the corrected values of strain and strain rate in the gage. This iterative refinement was continued until the change in values was within $\delta < 0.001$. The analytical calculations that gave corrected values of gage strain and strain rate and the iterative refinement of constitutive coefficients were performed using the spreadsheet and solver tools of Microsoft Excel. Once the corrected values of strain and strain rate were calculated, the iterative refinement method was performed to establish the constitutive coefficients. The refined values of the constitutive coefficients for the various strain rates are presented in Table 3.

3.2 Tensile Test Correlation

A set of interrupted tensile tests was conducted on gridded tensile specimens in order to measure the true strain in the gage. The specimens were strained to 15, 30, 50, and 100% tensile elongation for two different jump tests: 1×10^{-3}/s to 2×10^{-3}/s and 5×10^{-3}/s to 6×10^{-3}/s. The true strain in the gage section in each of these samples was measured using a toolmaker's microscope. The test samples are shown in Fig. 6. The measured values of strain were then compared to the values predicted by the analytical model.

Figure 7 shows a comparison of the true gage strain values predicted by the analytical model with measured values of true strain in the gage section of tensile specimens. The Figure also shows the uncorrected strain values which do not account for grip flow. The results shown in Fig. 7 correspond to two jump tests with initial strain rate values of 1×10^{-3}/s and 5×10^{-3}/s which were increased at 5% tensile elongation to 2×10^{-3}/s and 6×10^{-3}/s, respectively. The strain profiles that were predicted analytically correlated very well to the experimentally measured values.

3.3 Unified Constitutive Coefficients

While the analytical model is able to capture the effect of grip flow accurately, it generates multiple sets of constitutive coefficients corresponding to each tensile test. The ultimate

Table 3 Refined constitutive coefficients

Initial strain rate, s^{-1}	K, MPa	m	n
10^{-3}	261.6	0.42	0.149
2×10^{-3}	189.8	0.39	0.098
3×10^{-3}	169.8	0.37	0.095
4×10^{-3}	150.0	0.36	0.084
6×10^{-3}	139.8	0.34	0.077

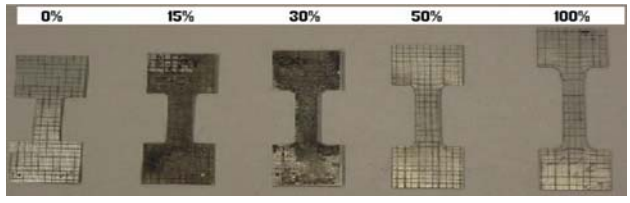

Fig. 6 Tensile specimens with 2.5 mm etched grid from interrupted jump tests (initial strain rate 10^{-3}) shown here in the as received condition and tested to 15, 30, 50, and 100% tensile elongation

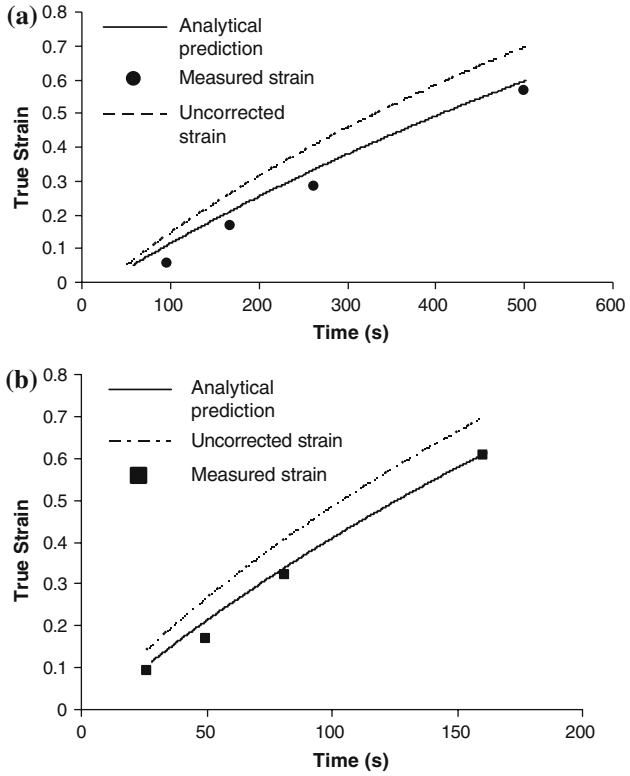

Fig. 7 True strain vs. time comparing the strain values predicted by the analytical model and FE simulation and measured values from experiment to uncorrected values of strain corresponding to two post jump strain rates of (a) 2×10^{-3}/s (b) 6×10^{-3}/s

utility of a constitutive equation is to model the complex process of superplastic forming where the strain rate can vary over a range depending on the features of the part. The range of strain rates that may be encountered during superplastic forming and the complexity involved in using multiple sets of coefficients to model the process necessitated the need for 'unified' constitutive coefficients that are valid for a specific range of strain rates. An analytical method was developed to obtain these so-called unified coefficients. In this study, the strain rate range was chosen to be from 10^{-3}/s to 3×10^{-3}/s which is a range typical of conventional automotive SPF.

The unified constitutive coefficients were calculated based on the corrected tensile data of all the tensile tests that fall within the strain rate range. Using the corrected strain and strain rate and a set of trial constitutive coefficients, the flow stress was calculated. The *m*-value for the trial coefficients was obtained by averaging all the *m*-values corresponding to the strain rates within the range. The actual values of flow stress were calculated from the load values and the cross-sectional areas which were calculated from the corrected values of strain. The square of the difference between the two flow stress values was calculated and the same was done for all the tensile data within the strain rate range. A minimization of all the sums of squares was performed keeping *m* constant and varying *K* and *n*. Using this approach a new, more general set of constitutive coefficients was obtained. These coefficients corresponded to a range of strain rates. The minimization was carried out for all data points that fell within 0.05 to 0.35 range of true strain. This range was chosen because these strains also represent strain levels that are common in SPF automotive products. The strain range was used in all the curve fitting operations performed in this work. The unified constitutive coefficients are shown in Table 4.

The unified constitutive coefficients were used to analytically obtain load curves for the two non-jump tensile tests (initial strain rates 10^{-3}/s and 3×10^{-3}/s) using the method discussed in Section 3.2. These load curves were compared to the experimental load curves for the respective strain rates and showed good correlation. The results of the comparison are shown in Fig. 8 and 9. The application of the unified material model to simulation of automotive SPF and experimental correlation are discussed in Section 4.

4. Forming Trials

The geometry used in this SPF correlative study was a long rectangular cavity. The cavity had a length of 600 mm, width of 200 mm, and a depth of 100 mm. The entry radius was 10 mm, the die corner radius was 20 mm and there was a 5 degree draft angle. A CAD model of the die used to form the geometry is shown in Fig. 10.

4.1 Finite Element Analysis

Finite element analysis (FEA) was used to simulate the superplastic forming of the geometry in Fig. 10 and the predicted results were compared to experimental forming trials. The commercial FEA code LS-DYNA was used to simulate the process. The FEA model of the die-blank system with reduced

Table 4 Unified constitutive coefficients for strain rates between 1×10^{-3}/s and 3×10^{-3}/s

K, MPa	*m*	*n*
182.57	0.39	0.09

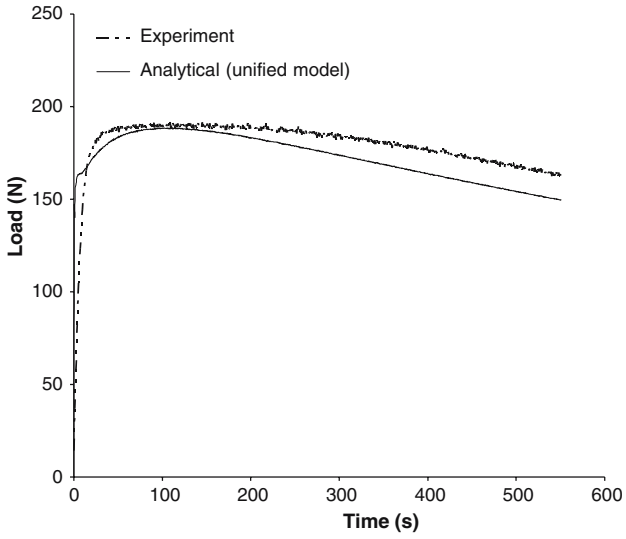

Fig. 8 Experimental load versus time curve compared to analytically derived load curve based on the unified constitutive model for lower bound strain rate 10^{-3}/s

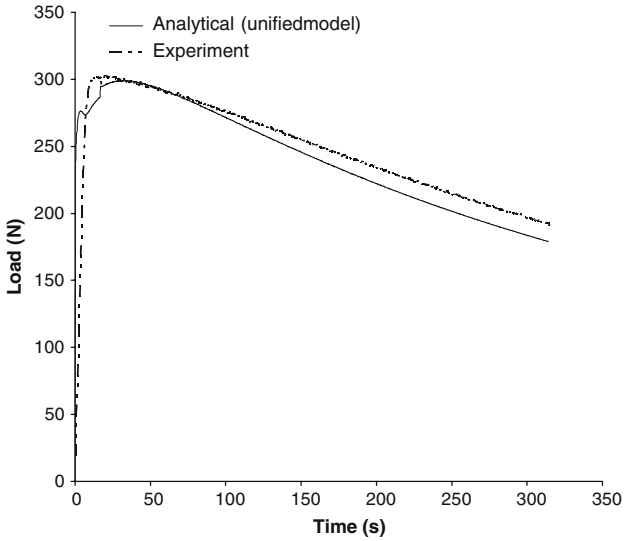

Fig. 9 Experimental load versus time curve compared to analytically derived load curve based on the unified constitutive model for upper bound strain rate 3×10^{-3}/s

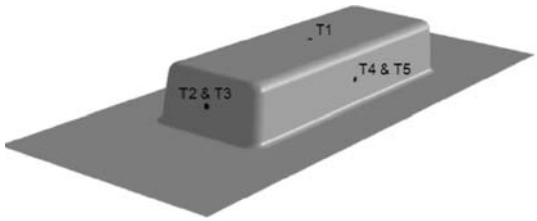

Fig. 10 A CAD model of the long rectangular cavity showing the points at which the thickness was measured and compared to the values predicted by FEA (Ref 2, 3)

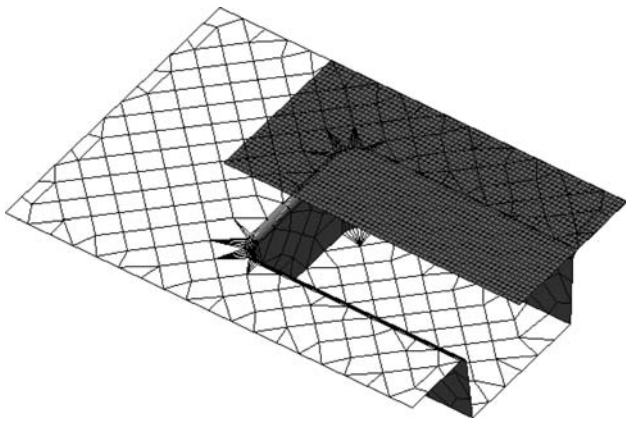

Fig. 11 A half section of the SPF die and a quarter section of the aluminum sheet was used to simulate the forming of the long rectangular cavity

integration shell elements was used to simulate the forming trials is shown in Fig. 11.

A viscoplastic formulation of the constitutive model shown in Eq 1 was applied in the FEA code. The contact between the sheet and the die was defined using surface to surface contact in the LS-DYNA code. The Coulomb friction model given by Eq 6 was used to define friction. The coefficient of friction has been reported to be reasonably approximated by 0.16 (Ref 2) and was used in all the FEA simulations.

$$\tau = \mu P \qquad \text{(Eq 6)}$$

The pressure cycle that was used in the experimental forming trials form the panel at a strain rate of 10^{-3}/s and were imported to LS-DYNA from the computer that was used to control the press. The cycle had been previously developed using a pressure prediction algorithm of LS-DYNA. The simulations were executed and the thickness profile of the sheet at specific points and the height to which the sheet had advanced into the die were monitored and the results were compared to experiment.

4.2 Experimental Setup

The forming trials were all done with an 800 ton superplastic forming press. The final part was obtained by forming the sheet up into the die cavity. The die was connected to the gas management system of the press and the pressure time curve for the forming cycle was controlled by the computer and the gas management system. The press was equipped with cartridge heaters to maintain the die halves at the required temperature. Thermocouples were used to monitor the temperature of the die halves. All the forming trials in this work were carried out within 3 °C of the target temperature of 475 °C.

The aluminum AA5083 sheets that were used for this study were all from the same batch of material. They were sheared to size and spray coated with a special Ford Motor Company proprietary solid lubricant. The purpose of the lubricant was to prevent material from sticking to the die and facilitate part removal. The sheet was preheated for 2 min prior to forming in a specially designed conduction heater. This preheat system rapidly raises the temperature of the sheet to the target forming temperature. It was reported by Friedman et al. (Ref 5) that the rapid preheating to target forming temperature resulted in a fully recrystallized, fine and equiaxed grain structure. The sheet was then automatically loaded into the press and positioned in order to allow the die halves to close and seal the forming cavity.

4.3 Forming Results

Parts were formed to intermediate positions in order to measure the height to which the center of the sheet had advanced into the die at a particular point in time. The final thickness profile was measured using an ultrasonic thickness gage at the center points of each face as shown in Fig. 10. The results predicted by FEA were then compared to the experimental values. A plot comparing the form heights predicted by FEA and experimental values is shown in Fig. 12.

Good correlation in thickness prediction between simulation and experiment was achieved for a maximum difference of no greater than 5% between predicted and experimentally measured thinning. The correlation in bulk sheet deformation into the cavity is considered good when the difference between the predicted and experimental sheet bulge height is less than 5 mm.

The percent thinning (e) was calculated using Eq 7, where t_f is the current thickness and t_o is the starting material thickness.

The percent thickness reduction at the different locations for a fully formed part is tabulated in Table 5. The thickness values predicted by FEA using the unified constitutive equation are also tabulated.

$$e = \frac{t_f - t_o}{t_o} \times 100 \quad \text{(Eq 7)}$$

The results show accurate prediction of the thickness profile on the part; however, the deformation of the sheet into the press is not captured accurately by the unified constitutive equation. This indicates an incorrect prediction of flow stresses as the sheet deforms into the die. The accurate prediction of the thickness profile indicates that the values of m and n are reasonably accurate since they have the strongest influence in thickness prediction. However, the K term of Eq 1 acts as a stress amplitude and is the dominant coefficient influencing flow stress in the material model. These results suggest that additional adjustment of K is needed to accurately describe the sheet deformation into the die.

5. Discussion

The unified constitutive model was derived based on high temperature tensile tests although their primary utility will be in the simulation of superplastic forming. There exist significant differences in the operating conditions between a high temperature tensile test and a part forming trial in an SPF press. The tensile specimen was subject to a 90 min preheat cycle before the crosshead moved to commence the tensile test. The aluminum sheet was rapidly heated to the target temperature for 2 min in a contact preheater. It has been reported in previous research that the AA5083 alloy experiences static grain growth when exposed to superplastic temperatures that change the constitutive behavior (Ref 5, 6). The difference in the exposure time to superplastic temperatures was hypothesized to have resulted in differences between the microstructural state of the tensile specimen and the gas formed aluminum sheet. If this hypothesis is true, the development of the material model must consider the difference in initial grain size due to pre-heat duration and its influence on the flow behavior.

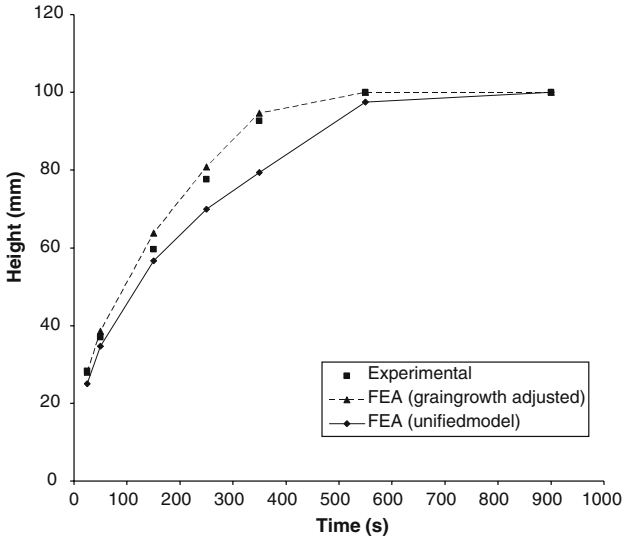

Fig. 12 Plot comparing the height vs. time curve predicted by FEA to experimental values at specific points in time at the center of the long rectangular cavity

Table 5 Percentage thickness reduction for values

	% Thinning		
Location	Experiment	FEA (unified model)	FEA (unified with grain growth)
T1	−38.27	−40.07	−38.63
T2 + T3	−43.6	−42.61	−42.82
T4 + T5	−40.57	−43.82	−44.37

An evaluation of the microstructural states of the tensile specimen and the aluminum sheet after the respective heat up cycles was carried out. Samples were cut from test blanks that were rapidly preheated to 475 °C over a period of 2 min which represented the typical heat up time during a superplastic forming cycle. Samples were cut both in the L-S (rolling direction × thickness) and T-S (transverse to rolling direction × thickness) orientations. The samples were hot mounted, polished manually and etched with Graf Sergeant reagent (Ref 4). In a similar manner, hot mounts were prepared using samples taken from a tensile specimen that was statically suspended in the load frame furnace to simulate the heating time of a tensile test. These samples were subject to a metallographic analysis to examine whether or not static grain growth occurred. The metallographic samples were observed under a microscope and an average grain size was calculated using the mean liner intercept method. Digital micrographs of the samples from the two different conditions are shown here in Fig 13 and 14.

The average grain size for an exposure time of 2 min was found to be 6.6 μm from a total of 3300 grains. Similarly, for an exposure time of 90 min the average grain size was found to be 7.8 μm from a total of 2800 grains. Thus, the difference in average static grain growth was calculated to be 1.2 μm. Since grain growth directly influences flow stress, the flow stresses in the material with the larger average grain size is expected to be greater than the flow stress values in the material with the average smaller grain size. The constitutive model that was analytically refined was based on tensile data and applied well to the tensile test simulations showing good correlation to

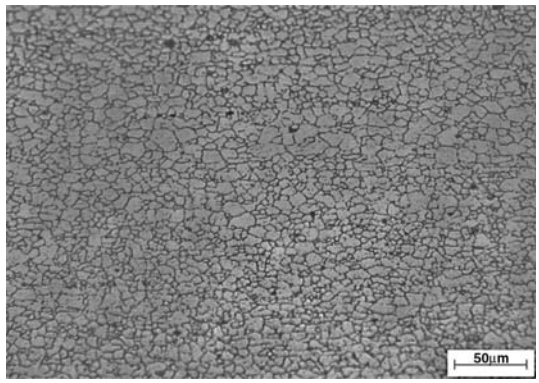

Fig. 13 Micrograph of metallographic sample obtained from a sheet that was preheated to 475 °C over a period of 2 min

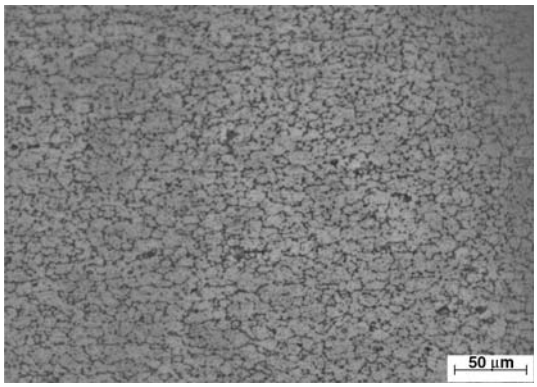

Fig. 14 Micrograph of metallographic sample obtained from tensile specimen that was statically suspended in a furnace and exposed to a surrounding temperature of 475 °C for 90 min

experiment. However, to accurately simulate SPF, this model must be further refined to account for the difference in the microstructures (Ref 6).

The difference in heat exposure times was assumed to have a negligible effect on strain hardening and strain rate sensitivity since the prediction of thickness profile was accurate. To validate this hypothesis, small changes in m and n were made to the power law equation in the FEA code and were found to have negligible influence on the final prediction of thickness distribution or the deformation characteristics of the sheet. The flow stress adjustment was achieved by adjusting the value of K based on a flow stress-grain growth relationship analytically derived from a mechanistic model for high temperature creep (Ref 6). The model is given by Eq 8.

$$\dot{\varepsilon} = \frac{ADG\vec{b}}{kT}\left(\frac{\vec{b}}{d}\right)^{p}\left(\frac{\sigma}{G}\right)^{c} \quad \text{(Eq 8)}$$

where D is the appropriate diffusion coefficient, $\dot{\varepsilon}$ is the strain rate, G is the shear modulus, $\vec{b}$ is the Burgers vector, k is the Boltzmann's constant, d is the grain size, σ is the applied stress, p is the exponent of inverse grain size, c is a stress exponent, and A is a dimensionless constant. Two hypothetical tensile tests with specimens having different initial average grain sizes were considered. With all other conditions remaining the same, A, D, G, $\vec{b}$, k, and T were the same for both these tests. Thus, for a given strain rate value, the flow stress ratio as a function of grain size ratio is given by Eq 9.

$$\left(\frac{\sigma_1}{\sigma_2}\right)^{c} = \left(\frac{d_1}{d_2}\right)^{p} \quad \text{(Eq 9)}$$

The values of the exponents (c and p) were assumed to be 2 (Ref 5, 6). For the same two hypothetical tensile tests, the power law equation given by Eq 1 is used to derive a relationship between the flow stress and the K coefficient. For the same strain and strain rate, the relation is given here by Eq 10.

$$\frac{K_1}{K_2} = \frac{\sigma_1}{\sigma_2} \quad \text{(Eq 10)}$$

where K_1 and K_2 are the strength coefficients corresponding to the two hypothetical tests and σ_1 and σ_2 are the respective flow stress values. The grain sizes for the samples with a 2 min preheat time and 90 min of heat exposure were 6.6 µm and 7.8 µm, respectively. The flow stress ratio, $\sigma_{2min}/\sigma_{90min}$ was calculated to be 0.85. Based on Eq 4, 5 the K coefficient in the unified constitutive model was adjusted. The resulting coefficients are shown in Table 6.

Table 6 Constitutive coefficients after adjustment of K based on static grain growth

K, MPa	m	n
155.14	0.39	0.09

The unified model adjusted for static grain growth was used to simulate the SPF of the rectangular cavity. The form height plotted as a function of time is shown in Fig. 12. The thickness prediction of FEA is compared to experimental values in Table 5. The results show good correlation between FE prediction of form height and experimental values. Since m and n were not altered, the thickness prediction remains close to experimentally measured values. These results reinforce the need for accounting for the difference in microstructures in the constitutive model to achieve accurate simulation of the process.

6. Summary and Conclusions

The parameters of the constitutive equation are typically derived from high temperature tensile test data. Due to the low flow stresses at superplastic temperatures, significant material flow from the grips to the gage section of the specimen occurs as the test progresses. This flow of material induces significant error into the calculation of the strain and strain rate. Thus, the superplastic material parameters calculated without accounting for flow of material from the grips of the specimen fail to represent the deformation behavior of the material.

An investigation into the microstructure of the alloy revealed different grain sizes in the tensile test specimen and the aluminum sheet that was formed in the press. The long heat up cycle (90 min) in the case of the tensile specimen resulted in static grain growth that was absent in the aluminum sheet that was rapidly heated by a preheater to the forming temperature. The static grain growth resulted in higher values of flow stress in case of the tensile specimen. Refined material model parameters were then calculated and used to simulate superplastic tensile tests. The refined material constitutive model which took into account the effect of grain growth during the heating phase of the uniaxial tensile test, and material flow from the grips provided the ability to accurately predict the thickness distribution and evolution of part shape.

References

1. N. Chandra, Constitutive Behavior of Superplastic Materials, *Int. J. Non-Linear Mech.*, 2002, **37**, p 461–484
2. S.G. Luckey, "Development of Finite Element Analysis Based Tools and Methods for Design of Advanced Superplastic Forming Dies or Processes", PhD dissertation, Michigan Technological University, 2006

3. P.A. Friedman and A.K. Ghosh, Control of Superplastic Deformation Rate during Uniaxial Tensile Tests, *Metall. Mater. Trans. A*, 1996, **27A**, p 3030–3042
4. P.A. Friedman and W.B. Copple, Superplastic Response in Al-Mg Sheet Alloys, *J. Mater. Eng. Perform.*, 2004, **13**(3), p 335–347
5. P.A. Friedman, W.B. Copple, "Characterization of Superplastic Response in Al-Mg Alloys", Ford R & A Technical Report, SRR-2002-076, 2002
6. T.G. Langdon, A Unified Approach to Grain Boundary Sliding in Creep and Superplasticity, *Acta Metall. Mater.*, 1994, **42**(7), p 2437–2443